Galileo AltBOC E5 signal characteristics for optimal tracking algorithms

Petr Kačmařík, Pavel Kovář, František Vejražka

Czech Technical University in Prague, Faculty of Electrical Engineering
Prague 166 27, Czech Republic
kacmarp@fel.cvut.cz

***Abstract*—The paper shows an analytical derivation of the cross correlation function (CCF) of two AltBOC modulated signals, which differ in their data bits sequences (have different navigation messages) or in their secondary code phases. The final equation for CCF is general in such ways, that the arbitrary integration time and data bits sequences combinations can be considered. Such formula thus covers all possibilities which are needed for the tracking loop detector design. The theoretical results were approved with a numerical simulation.**

The structure of the new delay loop detector based on the results of discussion is proposed. The tracking algorithms based on the proposed structure therefore fully utilize capability of the Galileo wideband E5 signal.

***Index Terms*—Galileo, E5 signal, AltBOC multiplex**

I. Introduction

The NEW European satellite navigation system Galileo promises remarkable performance by means of the wideband E5 signal.

The Galileo E5 signal is formed through AltBOC multiplex, which gathers four input signals (two pilots and two data signals) to form the output wideband complex E5 signal. Such modulation scheme is rather complicated and has no similarity in currently deployed GNSS (GPS, GLONASS). Therefore the notably modified signal tracking algorithm must be used to utilize full E5 signal capability.

There are some works which solve the E5 signal tracking problem and propose tracking algorithms (e.g. [1]). Unfortunately, such tracking algorithms do not fully utilize wideband E5 signal capability, mostly due to their simplifying assumptions (e.g. using AltLOC [Linear offset carrier] counterpart instead of full-valued AltBOC). Our work overcomes this lack and presents the tracking algorithm based on correctly derived E5 signal characteristics.

The loop detector can be understood as a core of the tracking loop. The tracking performance is bounded with loop detector characteristics. Since the loop detector characteristics are formed with the cross-correlation function (CCF) between the received signal and the generated replica, the E5 CCF is the focus of our attention.

The E5 CCF has significant dependency on data bits sequences in both the received signal and the generated replica which are carried on E5aI and E5bI AltBOC input components. The bits disagreement in the received signal and the replica has a negative effect on the CCF maximum height and therefore also on the tracking performance. The similar effect has also the secondary codes nonsynchronization. The described situation becomes more complicated with the integration time increase since more data bits (secondary code chips) combinations should be taken into a consideration.

II. Theoretical background

The property of navigation signal should ensure effective ranging measurement and also minimal interference with navigation signals from other satellites. Therefore the navigation signals are based on pseudorandom sequences (codes) which ensure proper correlation characteristics for ranging measurement and also orthogonality with other navigation signals.

The signal correlation properties will be main topic of this section. The goal is to introduce appropriate system of correlation characteristics which can be used for a complicated navigation signal analysis.

A. Correlation function definitions

The pseudorandom sequence is discrete time periodic signal. It will be shown, that the correlation characteristics definition is more convenient if it is based on finite sequence than on periodic one. Such finite sequence is defined as a just one period of its periodic counterpart.

For two real finite sequences $a_1[k]$ and $a_2[k]$ with length N (the $a_1[k]$ and $a_2[k]$ are zero outside the interval $\langle 0, N-1\rangle$) we can define so called linear cross correlation function (CCF) as follow

$$\rho_{a,12}[m] = \sum_{k=-\infty}^{\infty} a_1[k]\, a_2[k+m] \tag{1}$$

Since the sequences have finite length the CCF is finite too (the $\rho_{a,12}[m]$ is zero outside interval $\langle -N+1, N-1\rangle$). The so called circular CCF is defined as

$$\mathcal{R}_{a,12}[m] = \frac{1}{N}\sum_{k=0}^{N-1} \ddot{a}_1[k]\, \ddot{a}_2[k+m] \tag{2}$$

where $\ddot{a}_i[k] = \sum_{l=-\infty}^{\infty} a_i[k-lN]$ is a periodic extension of finite sequence $a_i[k]$. The circular CCF is periodic with the identical period N as the periodic extension $\ddot{a}_i[k]$. The significant property of these CCF definitions is the fact that we can easily derived $\mathcal{R}_{a,12}[m]$ from $\rho_{a,12}[m]$ (but contrary way is not possible)

$$\mathcal{R}_{a,12}[m] = \frac{1}{N} \sum_{l=-\infty}^{\infty} \rho_{a,12}[m - lN] \tag{3}$$

It is also important to outline the connection with continuous time signals and their correlation characteristics. The continuous time signal $a_i(t)$ derived from the finite sequence $a_i[k]$ can be constructed as $a_i(t) = \sum_{k=0}^{N-1} a_i[k] g_{T_c}(t - kT_c)$ and its periodical extension as $\ddot{a}_i(t) = \sum_{l=-\infty}^{\infty} a(t - lT_c) = \sum_{k=-\infty}^{\infty} \ddot{a}_i[k] g_{T_c}(t - kT_c)$. Since one element of pseudorandom sequence is usually denoted as chip the constant T_c is than one chip duration. Through the pulse $g_{T_c}(t)$ we can easy consider impact of finite channel bandwidth. In ideal case, when we can consider infinite channel bandwidth the rectangular shape with duration T_c is used.

In similar manner as in sequence case we can define linear and circular CCF for continuous time counterpart as following

$$\rho_{a,12}(\tau) = \int_{-\infty}^{\infty} a_1(t)\, a_2(t + \tau)\, \mathrm{d}t \tag{4}$$

$$\mathcal{R}_{a,12}(\tau) = \frac{1}{NT_c} \int_{0}^{NT_c} \ddot{a}_1(t)\, \ddot{a}_2(t + \tau)\, \mathrm{d}t \tag{5}$$

The important is a mutual relation between particular CCF definitions. It can be derived (see [3] for more details)

$$\rho_{a,12}(\tau) = \sum_{m=-\infty}^{\infty} \rho_{a,12}[m] \rho_{g_{T_c}}(\tau - mT_c) \tag{6}$$

$$\begin{aligned}\mathcal{R}_{a,12}(\tau) &= \frac{1}{NT_c} \sum_{m=-\infty}^{\infty} \rho_{a,12}(\tau - mNT_c) = \\ &= \frac{1}{T_c} \sum_{m=-\infty}^{\infty} \mathcal{R}_{a,12}[m]\, \rho_{g_{T_c}}(\tau - mT_c) \end{aligned} \tag{7}$$

where $\rho_{g_{T_c}}(\tau)$ is the autocorrelation function (ACF) of $g_{T_c}(t)$ defined as $\int_{-\infty}^{\infty} g_{T_c}(t)\, g_{T_c}(t + \tau)\, \mathrm{d}t$. In ideal case when the infinite channel bandwidth is considered, the $\rho_{g_{T_c}}(\tau)$ has triangular shape.

The remarkable consequence of previous equations is the fact, that the $\rho_{a,12}[m]$ can be considered as the most universal characteristic in the case of the correlation properties investigation. From the $\rho_{a,12}[m]$ we can easily calculate all other CCF – $\mathcal{R}_{a,12}[m]$, $\rho_{a,12}(\tau)$ and $\mathcal{R}_{a,12}(\tau)$.

B. Ideal pseudorandom sequence

For navigation signal description we need some appropriate approximation of pseudorandom sequences. The correlation function of sequence depends on sequence itself, this dependency can cause some inconvenience during analytical derivation. Therefore we introduce the ideal pseudorandom sequence as a hypothetical sequence defined only by its correlation characteristics. Correlation properties of such sequence well represent all pseudorandom sequences with length N.

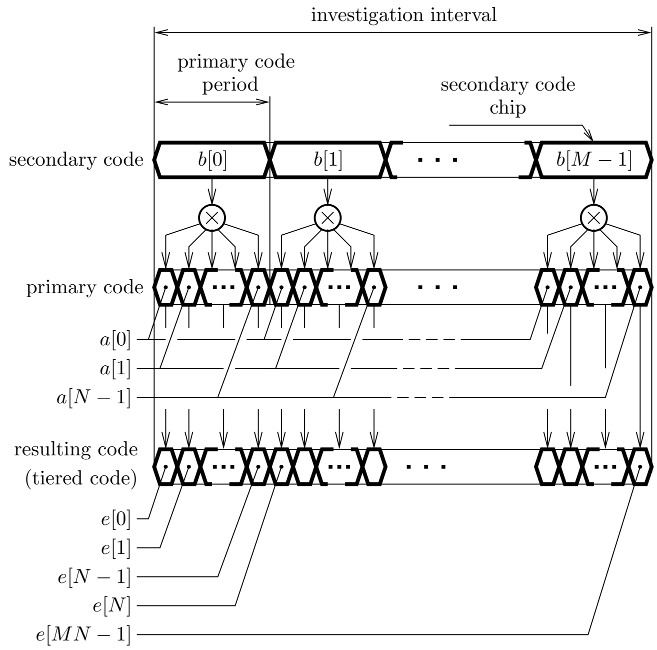

Figure 1. The tiered sequence construction

The CCF of ideal pseudorandom sequence is defined as follows

$$\rho_{I,ij}[m] = \begin{cases} N\delta[m] & \text{for } i = j, \\ 0 & \text{otherwise} \end{cases} \tag{8}$$

where $\delta[m]$ is the unit impulse function.

C. Tiered sequence

The tiered sequence is published in Galileo ICD [2]. The construction of tiered sequence offers a technique which enables the combination of two pseudorandom sequences to get sequence with large length (period). The tiered sequence generation is based on two independent sequences: the primary sequence $a[k]$ with length N and the secondary sequence $b[k]$ with length M. The resulting tiered sequence, we denote it as $e[k]$, has length MN.

The construction of tiered sequence $e[k]$ is shown in Fig. 1. The $a[k]$ is M times repeated and lined up. The i-th $a[k]$ segment with length N is then multiplied by i-th chip of $b[k]$.

It is possible to derive a formula which computes CCF of tiered sequences based solely on CCF of its primary and secondary sequences (detailed derivation is also in [3])

$$\rho_{e,12}[m] = \sum_{l=-\infty}^{\infty} \rho_{b,12}[l]\, \rho_{a,12}[m - lN] \tag{9}$$

Using this equation together with (3) we can also get

$$\mathcal{R}_{e,12}[m] = \frac{1}{N} \sum_{l=-\infty}^{\infty} \mathcal{R}_{b,12}[l]\, \rho_{a,12}[m - lN] \tag{10}$$

The other CCF can be computed according equations in section II-A.

The equations (9) and (10) offer a suitable tool for the complicated navigation signals analysis. Of course, the navigation signal structure must allow its decomposing into separate sequences and to arrange them according Fig. 1. Then we can investigate the separated sequences independently and use the (9) and (10) together with equations from section II-A for this complicated navigation signal characteristics. The outlined method can be generalized for arbitrary number of tiers.

III. Galileo E5 signal

A. Galileo E5 signal parameters

The wideband Galileo E5 signal is composed using AltBOC multiplex from four independent signals which are usually denoted as E5aI, E5aQ, E5bI and E5bQ. Each of this multiplex inputs has pseudorandom sequence constructed as a tiered code. Signals E5aI and E5bI are further BPSK modulated with navigation message, signals E5aQ and E5bQ have no modulation and therefore are called as pilot signals. The parameters of the E5 multiplex inputs are gathered in Tab. I.

B. AltBOC multiplex

Due to the comfortable mathematical description we denote AltBOC multiplex inputs as $e_i[k]$ where index stands for ith multiplex input (1 E5aI, 2 for E5aQ, etc.) Apart inputs $e_i[k]$ the multiplex output is also based on two subcarriers denoted as $sc_s[k]$ and $sc_p[k]$. However, these subcarriers are quicker than $e_i[k]$. Therefore to satisfy right timing relation the inputs $e_i[k]$ must be oversampled by $S = 12$, where the S is the number of subcarrier samples per one primary sequence chip. The oversampled inputs we denote as $\varepsilon_i[k]$. The multiplex output is defined in Galileo ICD [2] with equation (3). We adjust this definition to agree with our notation. The AltBOC output sequence can than be written as

$$\begin{aligned}\mathcal{E}5[k] = \frac{\sqrt{P}}{2\sqrt{2}}\times \\ &\Big\{\big(\varepsilon_1[k] + \mathrm{j}\varepsilon_2[k]\big)\big(sc_s[k] - \mathrm{j}sc_s[k-2]\big) + \\ &+ \big(\varepsilon_3[k] + \mathrm{j}\varepsilon_4[k]\big)\big(sc_s[k] + \mathrm{j}sc_s[k-2]\big) + \\ &+ \big(\bar{\varepsilon}_1[k] + \mathrm{j}\bar{\varepsilon}_2[k]\big)\big(sc_p[k] - \mathrm{j}sc_p[k-2]\big) + \\ &+ \big(\bar{\varepsilon}_3[k] + \mathrm{j}\bar{e}_4[k]\big)\big(sc_p[k] + \mathrm{j}sc_p[k-2]\big)\Big\} \qquad (11)\end{aligned}$$

where P stands for $\mathcal{E}5[k]$ signal power. The bar signal $\bar{\varepsilon}_i[k]$ for ith input branch is computed as a multiplication of all other inputs, e.g. $\bar{\varepsilon}_1 = \varepsilon_2[k]\varepsilon_3[k]\varepsilon_4[k]$.

IV. Galileo E5 signal correlation characteristics

In DLL detector the mutual signal power between the received signal and the locally generated replica is computed over a fix integration time interval T_I. In mathematical description the mutual power for arbitrary signal delay can be expressed using following CCF

$$\mathcal{R}_{^s\mathcal{E}5,^r\mathcal{E}5}(\tau) = \frac{1}{T_I}\int_{T_I} {^s\ddot{\mathcal{E}}5}^*(t)\,{^r\ddot{\mathcal{E}}5}(t+\tau)\,\mathrm{d}t \qquad (12)$$

The expression of this characteristic in suitable form is therefore primary goal of this section.

A. Problem description

The typical choice of the value T_I is interval which corresponds to integer multiple of primary sequence period duration. This integer multiple we denote as M (since primary code period duration is 1ms, then $T_I = M$ ms). Thus, in this section, M is not necessarily a period of secondary sequence but just a number of secondary sequence chips which are involved into integration over T_I.

The M is usually smaller than secondary sequence period. Consequently it cannot be ensured, that the received signal and the generated replica are based on identical chips of secondary sequences. It is necessary to distinguish them. The secondary sequence subset used in the received signal we denote as ${^s b_i}[k]$, in the locally generated replica as ${^r b_i}[k]$. To simplify the problem the navigation data bits can be included into corresponding b_i sequences without lost of generality (thus b_i for $i \in \{1,3\}$ is considered as secondary sequences multiplied by data bits). The received signal and generated replica can also differ in their powers, we denote them as ${^s P}$ and ${^r P}$.

We use the outlined concept from section II-A for solving (12). There was stated, it is sufficient to compute CCF from discrete signal representation, in our case from $\mathcal{E}5[k]$. Due to the subcarrier in AltBOC multiplex, the discrete step k cannot correspond to one chip duration T_c but smaller interval T_s. Since the ratio T_c/T_s is S and the period of primary sequence is N and number of secondary sequence chips used for integration is M, the CCF is computed over interval MNS

$$\mathcal{R}_{^s\mathcal{E}5,^r\mathcal{E}5}[m] = \frac{1}{MNS}\sum_{k=0}^{MNS-1} {^s\ddot{\mathcal{E}}5}^*[k]\,{^r\ddot{\mathcal{E}}5}[k+m] \qquad (13)$$

The method to solve (13) is based on decomposition of $\mathcal{R}_{^s\mathcal{E}5,^r\mathcal{E}5}[m]$ terms on the interval MNS into several tiers, so correlation properties of each tier can be investigated separately and resulting $\mathcal{R}_{^s\mathcal{E}5,^r\mathcal{E}5}[m]$ can be determined using rules from section II-C. The CCF (12), if needed, can be then easily constructed from (13) for arbitrary shape of pulse $g_{T_s}(t)$ using (7).

B. Sequences decomposition

After the (11) expansion we get terms in form of the multiplication ε_i or $\bar{\varepsilon}_i$ with one of the subcarriers sc_s or sc_p. We will do now some modification to transform these terms into suitable form for expressing them as tiered sequences.

1) AltBOC multiplex inputs decomposition: The AltBOC multiplex input sequence in ith branch is constructed as tiered sequence from $a_i[k]$ with length N in lower tier and $b_i[k]$ with length M in upper tier, see fig. 1. Formally $e_i[k]$ can be expressed as

$$e_i[k] = \sum_{l=0}^{M-1} b_i[l]\,a_i[k-lN] \qquad (14)$$

To satisfy the time relation with subcarrier, the $e_i[k]$ must be oversampled by S. Such oversampled sequence we denote as $\varepsilon_i[k]$

	primary seq.			secondary seq.	data	
	N [chip]	$1/T_c$ [chip/s]	NT_c [ms]	M [chip]	$1/T_d$ [sym/s]	T_d [ms]
E5aI e_1	10230	$1.023\,10^6$	1	20	50	20
E5aQ e_2	10230	$1.023\,10^6$	1	100	–	–
E5bI e_3	10230	$1.023\,10^6$	1	4	250	4
E5bQ e_4	10230	$1.023\,10^6$	1	100	–	–

Table I
GALILEO E5 ALTBOC MULTIPLEX INPUT SIGNALS PARAMETERS

$$\varepsilon_i[k] = \sum_{j=0}^{M-1} b_i[j] \sum_{l=0}^{N-1} a_i[l]\,\mathrm{Rect}_S[k - lS - jNS] \qquad (15)$$

where $\mathrm{Rect}_S[k] = \mathrm{Us}[k] - \mathrm{Us}[k-S]$ is the discrete rectangular pulse with length S, $\mathrm{Us}[k]$ is the discrete unit step function. The formulas for $\bar{e}_i[k]$ and $\bar{\varepsilon}_i[k]$ can be expressed in identical manner, only $\bar{a}_i[k]$ and $\bar{b}_i[k]$ have to be used.

2) Subcarriers decomposition: Sequences $sc_s[k]$ and $sc_p[k]$ are defined in Tab. 5 in Galileo ICD [2]. The $sc_s[k]$ represent coarsely quantized cosine waveform. The $sc_p[k]$ is designed in such way to ensure together with $\bar{\varepsilon}_i[k]$ a constant envelope of AltBOC output $\mathcal{E}5[k]$ (this correspond with last two line in equation (11)).

Sequences $sc_s[k]$ and $sc_p[k]$ are periodic with period 8. To use the proposed method from sec. II-C the finite sequences, which cover just one chip of $a_i[k]$, must be formed. Therefore we define $s_i[k]$ with length $S = 12$ as follows

$$s_1[k] = sc_s[k]\left(\mathrm{Us}[k] - \mathrm{Us}[k-S]\right) \qquad (16)$$

$$s_2[k] = sc_s[k-2]\left(\mathrm{Us}[k] - \mathrm{Us}[k-S]\right) \qquad (17)$$

$$s_3[k] = sc_p[k]\left(\mathrm{Us}[k] - \mathrm{Us}[k-S]\right) \qquad (18)$$

$$s_4[k] = sc_p[k-2]\left(\mathrm{Us}[k] - \mathrm{Us}[k-S]\right) \qquad (19)$$

The $s_i[k]$ and their relations to harmonic waveforms are clear from Fig. 2.

The original ICD subcarriers $sc_s[k]$ and $sc_p[k]$ can be from $s_i[k]$ formed only with help of sequence $z[k] = (-1)^k$. E.g. $sc_s[k]$ can be using $s_1[k]$ expressed as

$$sc_s[k] = \sum_{i=0}^{MN-1} z[i] s_1[k - iS] \qquad (20)$$

See Fig. 3 for better understanding. Thus $sc_s[k]$ was decomposed into two tiers, $z[k]$ in upper and $s_1[k]$ in lower. Similar decomposition can also be done for the $sc_s[k-2]$, $sc_p[k]$ and $sc_p[k-2]$.

Now we will show that z tier has no impact on correlation property and therefore can be omitted. The tier z is on the same level as $a_i[k]$ (the one $a_i[k]$ chip duration correspond with $z[k]$ element duration). We assume, the $a_i[k]$ can be well approximated with ideal pseudorandom sequence. The CCF of

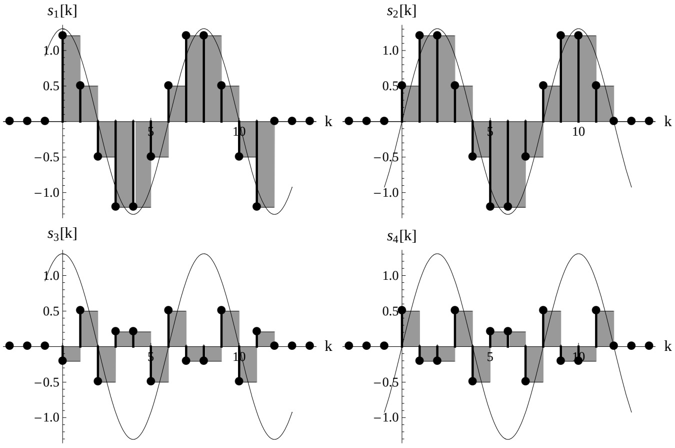

Figure 2. Construction of finite subcarrier sequences $s_i[k]$

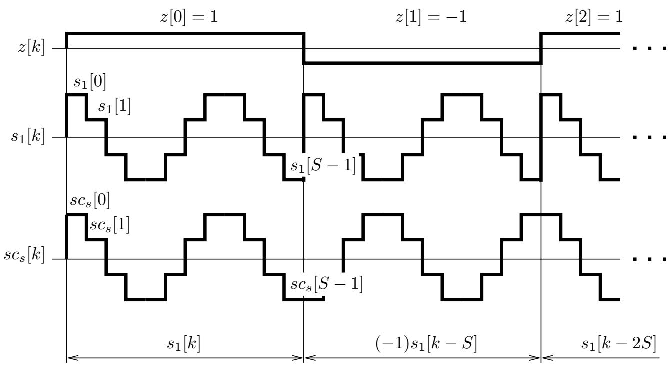

Figure 3. Decomposition of $sc_s[k]$ into $z[k]$ and $s_1[k]$

$a_i[k]z[k]$ and $a_j[k]z[k]$ is given as follows

$$\sum_{k=-\infty}^{\infty} a_i[k](-1)^k a_j[k+m](-1)^{k+m} = = (-1)^m \sum_{k=-\infty}^{\infty} a_i[k]a_j[k+m] = = (-1)^m \rho_{a,ij}[m] = \rho_{a,ij}[m] \qquad (21)$$

The last equality is a consequence of (8). Thus, CCF of $a_i[k]z[k]$ and $a_j[k]z[k]$ is identical with CCF of $a_i[k]$ and $a_i[k]$.

C. Subcarrier correlation matrix

The CCF (13) will be certainly depended on ACF/CCF of our defined subcarriers $s_i[k]$. We compute them now and show some their properties which will be helpful during next simplification.

For better manipulation with the subcarriers $s_i[k]$ we arrange them into row vector $\mathbf{s}[k] = (s_1[k], s_2[k], s_3[k], s_4[k])$. Then the subcarriers ACF/CCF matrix can be defined

$$\boldsymbol{\rho}_{\mathbf{s}}[m] = \sum_{k=-\infty}^{\infty} \mathbf{s}^T[k]\,\mathbf{s}[k+m] = \\ = \begin{pmatrix} \rho_{s,11}[m] & \cdots & \rho_{s,14}[m] \\ \vdots & \ddots & \vdots \\ \rho_{s,41}[m] & \cdots & \rho_{s,44}[m] \end{pmatrix} \quad (22)$$

The subcarriers can be divided into two groups according their symmetry. Let the first group contains $s_i[k]$ with property $s_i[k] = s_i[S-k-1]$ (it is valid for $i = 1$ a 3), second group $s_i[k]$ with $s_i[k] = -s_i[S-k-1]$ (valid for $i = 2$ and 4). It can be proved, that as a consequence of this symmetry we can write for ACF/CCF

$$\rho_{s,ij}[m] = \rho_{s,ji}[m] = \rho_{s,ji}[-m]. \quad (23)$$

in case of s_i and s_j are from the same group and

$$\rho_{s,ij}[m] = -\rho_{s,ji}[m] = \rho_{s,ji}[-m] \quad (24)$$

in case of s_i and s_j are from the different groups.

Such information is useful during a simplification. Since some elements in (22) matrix are identical or opposite, the result will depend on fewer number of $\rho_{s(ij)}[m]$ terms.

The computed $\rho_{s(ij)}[m]$ are shown in Fig. 4 and their exact values in Tab. II.

D. Outline of CCF derivation

The $\mathcal{E}5[k]$ can be expressed as a sum of 16 terms and each of these terms can be further expressed as tiered sequences with $e_i[k]$ (or $\bar{e}_i[k]$) in the upper tier and $s_j[k]$ in the lower tier. For (13) evaluation we multiply the ${}^s\ddot{\mathcal{E}}5^*[k]$ with the ${}^r\ddot{\mathcal{E}}5[k+m]$ and after product expansion we get 256 terms in following form

$$\frac{\sqrt{{}^sP}}{2\sqrt{2}}\,\frac{\sqrt{{}^rP}}{2\sqrt{2}} \sum_{k=0}^{MNS-1} {}^s\ddot{\varepsilon}_i[k]\,{}^r\ddot{\varepsilon}_j[k+m]\,\ddot{s}_k[k]\,\ddot{s}_l[k+m] \quad (25)$$

Such term represents a circular CCF between ${}^s\varepsilon_i[k]s_k[k]$ and ${}^r\varepsilon_j[k]s_l[k]$. Using (10) the equation (25) can be rewritten as follows

$$\frac{\sqrt{{}^sP}}{2\sqrt{2}}\,\frac{\sqrt{{}^rP}}{2\sqrt{2}}\,\frac{1}{S} \sum_{i=-\infty}^{\infty} \mathcal{R}_{{}^se_i,{}^re_j}[i]\,\rho_{s,kl}[m-iS] \quad (26)$$

Note, the e_i is not necessary just one of the $\{e_1[k],\ldots,e_4[4]\}$ but can also be one of the $\{\bar{e}_1[k],\ldots,\bar{e}_4[4]\}$. Similar notes also concern the symbols $a_i[k]$ and $b_i[k]$.

The reduction of total terms number can be achieved after considering the $\rho_{s,kl}[m]$ symmetry properties which were expressed with equations (23) and (24). Then the number of terms reduces 208.

Now we focus on the $\mathcal{R}_{{}^se_i,{}^re_j}[m]$. Since $e_i[k]$ is tiered sequence constructed from b_i and a_i the $\mathcal{R}_{{}^se_i,{}^re_j}[m]$ can be using (10) rewritten as follows

$$\mathcal{R}_{{}^se_i,{}^re_j}[m] = \frac{1}{N} \sum_{i=-\infty}^{\infty} \mathcal{R}_{{}^sb_i,{}^rb_j}[i]\,\rho_{a,ij}[m-iN] \quad (27)$$

We assume, that the $a_i[k]$ can be well approximated with ideal pseudorandom sequence defined in sec. II-B. Then the $\rho_{a,ij}[m]$ has property according (8). Thus, due to the noncorrelation of two different primary sequences the most of the terms are zero and total number of terms reduces to 24. The nonzero terms have a form

$$\mathcal{R}_{{}^se_i,{}^re_i}[m] = \sum_{i=-\infty}^{\infty} \mathcal{R}_{{}^sb_i,{}^rb_i}[i]\,\delta[m-iN] \quad (28)$$

Substituting (28) into (26) we get

$$\frac{\sqrt{{}^sP}}{2\sqrt{2}}\,\frac{\sqrt{{}^rP}}{2\sqrt{2}}\,\frac{1}{S} \sum_{i=-\infty}^{\infty}\sum_{j=-\infty}^{\infty} \mathcal{R}_{{}^sb_i,{}^rb_i}[j]\,\delta[i-jN]\,\rho_{s,kk}[m-iS] \quad (29)$$

which simplifies to

$$\frac{\sqrt{{}^sP}\,\sqrt{{}^rP}}{8}\,\frac{1}{S} \sum_{j=-\infty}^{\infty} \mathcal{R}_{{}^sb_i,{}^rb_i}[j]\,\rho_{s,kk}[m-jNS] \quad (30)$$

E. Final formula

Outlined procedure was accomplished in the *Mathematica* software with following final issue. The real part of the $\mathcal{R}_{{}^s\mathcal{E}5,{}^r\mathcal{E}5}[m]$ can be expressed as

$$\mathrm{Re}\{\mathcal{R}_{{}^s\mathcal{E}5,{}^r\mathcal{E}5}[m]\} = \frac{\sqrt{{}^sP}\,\sqrt{{}^rP}}{8}\,\frac{1}{S} \times \Big\{ \\ \sum_{j=-\infty}^{\infty} \Big(\mathcal{R}_{{}^sb_1,{}^rb_1}[j] + \mathcal{R}_{{}^sb_2,{}^rb_2}[j] + \mathcal{R}_{{}^sb_3,{}^rb_3}[j] + \mathcal{R}_{{}^sb_4,{}^rb_4}[j]\Big) \times \\ \times \Big(\rho_{s,11}[m-jNS] + \rho_{s,22}[m-jNS]\Big) + \\ \sum_{j=-\infty}^{\infty} \Big(\mathcal{R}_{{}^s\bar{b}_1,{}^r\bar{b}_1}[j] + \mathcal{R}_{{}^s\bar{b}_2,{}^r\bar{b}_2}[j] + \mathcal{R}_{{}^s\bar{b}_3,{}^r\bar{b}_3}[j] + \mathcal{R}_{{}^s\bar{b}_4,{}^r\bar{b}_4}[j]\Big) \times \\ \times \Big(\rho_{s,33}[m-jNS] + \rho_{s,44}[m-jNS]\Big) \Big\} \quad (31)$$

the imaginary part of the $\mathcal{R}_{{}^s\mathcal{E}5,{}^r\mathcal{E}5}[m]$ can be expressed as

$$\mathrm{Im}\{\mathcal{R}_{{}^s\mathcal{E}5,{}^r\mathcal{E}5}[m]\} = \frac{\sqrt{{}^sP}\,\sqrt{{}^rP}}{4}\,\frac{1}{S} \times \Big\{ \\ \sum_{j=-\infty}^{\infty} \Big(\mathcal{R}_{{}^sb_1,{}^rb_1}[j] + \mathcal{R}_{{}^sb_2,{}^rb_2}[j] - \mathcal{R}_{{}^sb_3,{}^rb_3}[j] - \mathcal{R}_{{}^sb_4,{}^rb_4}[j]\Big) \times \\ \times \rho_{s,12}[m-jNS] + \\ \sum_{j=-\infty}^{\infty} \Big(\mathcal{R}_{{}^s\bar{b}_1,{}^r\bar{b}_1}[j] + \mathcal{R}_{{}^s\bar{b}_2,{}^r\bar{b}_2}[j] - \mathcal{R}_{{}^s\bar{b}_3,{}^r\bar{b}_3}[j] - \mathcal{R}_{{}^s\bar{b}_4,{}^r\bar{b}_4}[j]\Big) \times \\ \times \rho_{s,34}[m-jNS] \Big\} \quad (32)$$

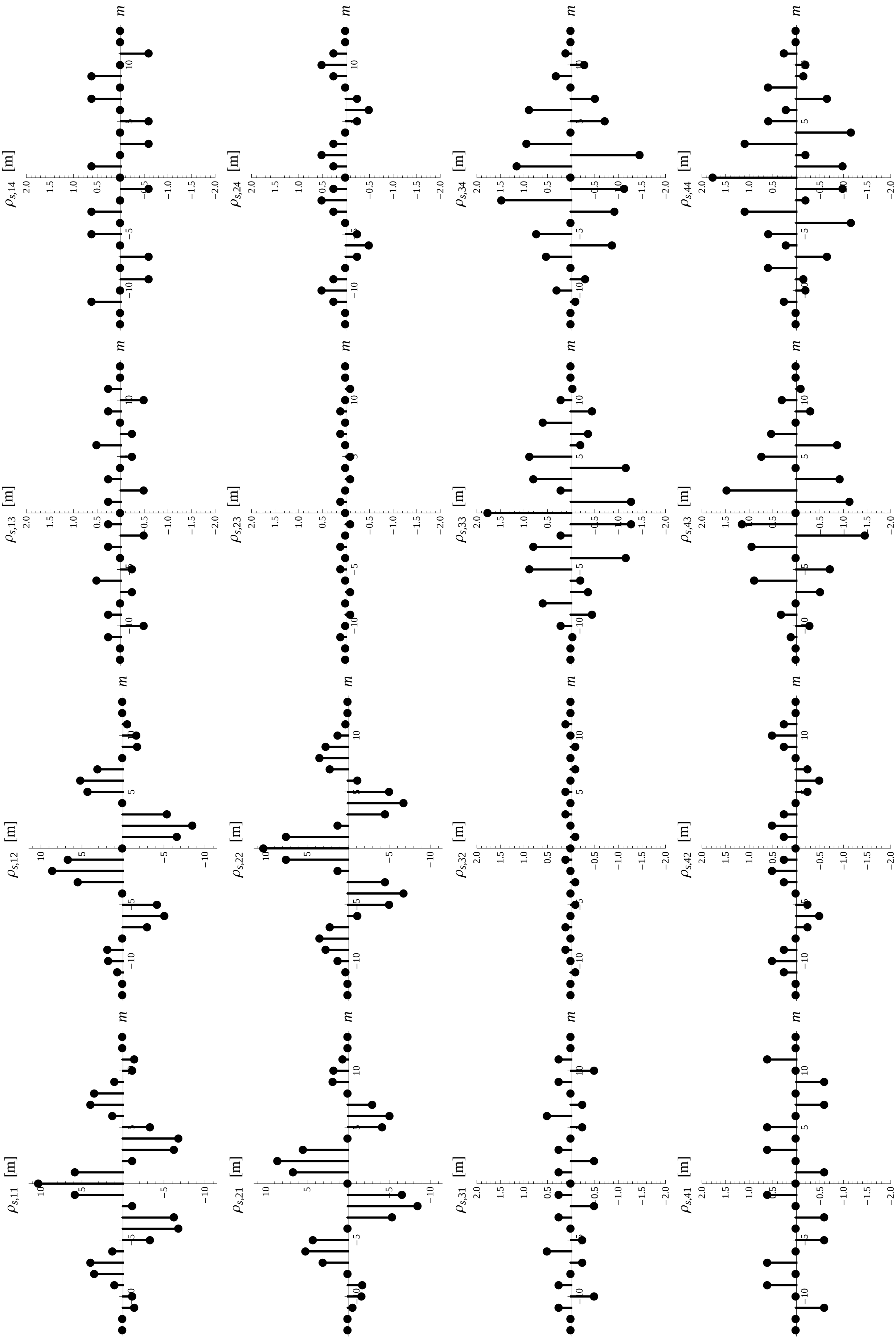

Figure 4. The charts of the subcarriers ACF/CCF

m	$\rho_{s,11}[m]$	$\rho_{s,22}[m]$	$\rho_{s,33}[m]$	$\rho_{s,44}[m]$	$\rho_{s,12}[m]$	$\rho_{s,34}[m]$
-12	0	0	0	0	0	0
-11	$-\frac{3}{4}-\frac{1}{\sqrt{2}}$	$\frac{1}{4}$	$-\frac{3}{4}+\frac{1}{\sqrt{2}}$	$\frac{1}{4}$	$\frac{1}{4}\left(1+\sqrt{2}\right)$	$\frac{1}{4}\left(1-\sqrt{2}\right)$
-10	$-\frac{1}{2}-\frac{1}{\sqrt{2}}$	$\frac{1}{2}+\frac{1}{\sqrt{2}}$	$-\frac{1}{2}+\frac{1}{\sqrt{2}}$	$\frac{1}{2}-\frac{1}{\sqrt{2}}$	$1+\frac{1}{\sqrt{2}}$	$1-\frac{1}{\sqrt{2}}$
-9	$\frac{1}{4}+\frac{1}{\sqrt{2}}$	$\frac{5}{4}+\sqrt{2}$	$\frac{1}{4}-\frac{1}{\sqrt{2}}$	$\frac{5}{4}-\sqrt{2}$	$\frac{3}{4}\left(1+\sqrt{2}\right)$	$-\frac{3}{4}\left(-1+\sqrt{2}\right)$
-8	$2+\sqrt{2}$	$2+\sqrt{2}$	$2-\sqrt{2}$	$2-\sqrt{2}$	0	0
-7	$\frac{7}{4}+\frac{3}{\sqrt{2}}$	$\frac{3}{4}+\sqrt{2}$	$\frac{7}{4}-\frac{3}{\sqrt{2}}$	$\frac{3}{4}-\sqrt{2}$	$-\frac{5}{4}\left(1+\sqrt{2}\right)$	$\frac{5}{4}\left(-1+\sqrt{2}\right)$
-6	$\frac{1}{2}+\frac{1}{\sqrt{2}}$	$-\frac{1}{2}-\frac{1}{\sqrt{2}}$	$\frac{1}{2}-\frac{1}{\sqrt{2}}$	$-\frac{1}{2}+\frac{1}{\sqrt{2}}$	$-\frac{3}{2}\left(2+\sqrt{2}\right)$	$-3+\frac{3}{\sqrt{2}}$
-5	$-\frac{5}{4}-\frac{3}{\sqrt{2}}$	$-\frac{9}{4}-2\sqrt{2}$	$-\frac{5}{4}+\frac{3}{\sqrt{2}}$	$-\frac{9}{4}+2\sqrt{2}$	$-\frac{7}{4}\left(1+\sqrt{2}\right)$	$\frac{7}{4}\left(-1+\sqrt{2}\right)$
-4	$-2\left(2+\sqrt{2}\right)$	$-2\left(2+\sqrt{2}\right)$	$2\left(-2+\sqrt{2}\right)$	$2\left(-2+\sqrt{2}\right)$	0	0
-3	$-\frac{11}{4}-\frac{5}{\sqrt{2}}$	$-\frac{7}{4}-2\sqrt{2}$	$-\frac{11}{4}+\frac{5}{\sqrt{2}}$	$-\frac{7}{4}+2\sqrt{2}$	$\frac{9}{4}\left(1+\sqrt{2}\right)$	$-\frac{9}{4}\left(-1+\sqrt{2}\right)$
-2	$-\frac{1}{2}-\frac{1}{\sqrt{2}}$	$\frac{1}{2}+\frac{1}{\sqrt{2}}$	$-\frac{1}{2}+\frac{1}{\sqrt{2}}$	$\frac{1}{2}-\frac{1}{\sqrt{2}}$	$5+\frac{5}{\sqrt{2}}$	$5-\frac{5}{\sqrt{2}}$
-1	$\frac{9}{4}+\frac{5}{\sqrt{2}}$	$\frac{13}{4}+3\sqrt{2}$	$\frac{9}{4}-\frac{5}{\sqrt{2}}$	$\frac{13}{4}-3\sqrt{2}$	$\frac{11}{4}\left(1+\sqrt{2}\right)$	$-\frac{11}{4}\left(-1+\sqrt{2}\right)$
0	$3\left(2+\sqrt{2}\right)$	$3\left(2+\sqrt{2}\right)$	$6-3\sqrt{2}$	$6-3\sqrt{2}$	0	0
1	$\frac{9}{4}+\frac{5}{\sqrt{2}}$	$\frac{13}{4}+3\sqrt{2}$	$\frac{9}{4}-\frac{5}{\sqrt{2}}$	$\frac{13}{4}-3\sqrt{2}$	$-\frac{11}{4}\left(1+\sqrt{2}\right)$	$\frac{11}{4}\left(-1+\sqrt{2}\right)$
2	$-\frac{1}{2}-\frac{1}{\sqrt{2}}$	$\frac{1}{2}+\frac{1}{\sqrt{2}}$	$-\frac{1}{2}+\frac{1}{\sqrt{2}}$	$\frac{1}{2}-\frac{1}{\sqrt{2}}$	$-\frac{5}{2}\left(2+\sqrt{2}\right)$	$-5+\frac{5}{\sqrt{2}}$
3	$-\frac{11}{4}-\frac{5}{\sqrt{2}}$	$-\frac{7}{4}-2\sqrt{2}$	$-\frac{11}{4}+\frac{5}{\sqrt{2}}$	$-\frac{7}{4}+2\sqrt{2}$	$-\frac{9}{4}\left(1+\sqrt{2}\right)$	$\frac{9}{4}\left(-1+\sqrt{2}\right)$
4	$-2\left(2+\sqrt{2}\right)$	$-2\left(2+\sqrt{2}\right)$	$2\left(-2+\sqrt{2}\right)$	$2\left(-2+\sqrt{2}\right)$	0	0
5	$-\frac{5}{4}-\frac{3}{\sqrt{2}}$	$-\frac{9}{4}-2\sqrt{2}$	$-\frac{5}{4}+\frac{3}{\sqrt{2}}$	$-\frac{9}{4}+2\sqrt{2}$	$\frac{7}{4}\left(1+\sqrt{2}\right)$	$-\frac{7}{4}\left(-1+\sqrt{2}\right)$
6	$\frac{1}{2}+\frac{1}{\sqrt{2}}$	$-\frac{1}{2}-\frac{1}{\sqrt{2}}$	$\frac{1}{2}-\frac{1}{\sqrt{2}}$	$-\frac{1}{2}+\frac{1}{\sqrt{2}}$	$3+\frac{3}{\sqrt{2}}$	$3-\frac{3}{\sqrt{2}}$
7	$\frac{7}{4}+\frac{3}{\sqrt{2}}$	$\frac{3}{4}+\sqrt{2}$	$\frac{7}{4}-\frac{3}{\sqrt{2}}$	$\frac{3}{4}-\sqrt{2}$	$\frac{5}{4}\left(1+\sqrt{2}\right)$	$-\frac{5}{4}\left(-1+\sqrt{2}\right)$
8	$2+\sqrt{2}$	$2+\sqrt{2}$	$2-\sqrt{2}$	$2-\sqrt{2}$	0	0
9	$\frac{1}{4}+\frac{1}{\sqrt{2}}$	$\frac{5}{4}+\sqrt{2}$	$\frac{1}{4}-\frac{1}{\sqrt{2}}$	$\frac{5}{4}-\sqrt{2}$	$-\frac{3}{4}\left(1+\sqrt{2}\right)$	$\frac{3}{4}\left(-1+\sqrt{2}\right)$
10	$-\frac{1}{2}-\frac{1}{\sqrt{2}}$	$\frac{1}{2}+\frac{1}{\sqrt{2}}$	$-\frac{1}{2}+\frac{1}{\sqrt{2}}$	$\frac{1}{2}-\frac{1}{\sqrt{2}}$	$-1-\frac{1}{\sqrt{2}}$	$-1+\frac{1}{\sqrt{2}}$
11	$-\frac{3}{4}-\frac{1}{\sqrt{2}}$	$\frac{1}{4}$	$-\frac{3}{4}+\frac{1}{\sqrt{2}}$	$\frac{1}{4}$	$\frac{1}{4}\left(-1-\sqrt{2}\right)$	$\frac{1}{4}\left(-1+\sqrt{2}\right)$
12	0	0	0	0	0	0

Table II
THE VALUES OF THE SUBCARRIERS ACF/CCF

F. Formula using and some consequences

One of the most important consequences is the ACF formula of the AltBOC signal. In this case there is no difference between ${}^{s}b_i[k]$ and ${}^{r}b_i[k]$ and thus $\mathcal{R}_{{}^{s}b_i,{}^{r}b_i}[m] = 1$ for $\forall m$. Similarly ${}^{s}P = {}^{r}P = P$. It is clear from (32), the imaginary part is zero. Since the (31) contains sum of four $\mathcal{R}_{{}^{s}b_i,{}^{r}b_i}[m] = 1$ and $S = 12$, the front constant can be evaluated as $\frac{\sqrt{P}\sqrt{P}}{8}\frac{1}{12}4 = \frac{P}{24}$ and ACF is then given

$$\mathcal{R}_{\mathcal{E}5}[m] = \frac{P}{24}\sum_{j=-\infty}^{\infty}\sum_{i=1}^{4}\rho_{s,ii}[m - jNS] \tag{33}$$

The $\mathcal{R}_{\mathcal{E}5}(\tau)$ can be constructed from $\mathcal{R}_{\mathcal{E}5}[m]$ using (7). The $\mathcal{R}_{\mathcal{E}5}(\tau)$ is shown in Fig. 5. The ideal situation with the infinite bandwidth channel is considered.

The equations (31) and (32) give unique possibilities for an impact investigation of both secondary code nonsynchronization and navigation data bits uncertainty. Let the integration time is restricted on 1ms (i.e. $M = 1$). Since AltBOC multiplex has four inputs branches there are sixteen possibilities of secondary sequences (dis)agreement in total and thus sixteen possible shapes of CCF. All of them are shown in Fig. 6, the secondary sequence agreement (disagreement) in particular AltBOC branch is indicate with 1 (-1) in charts title.

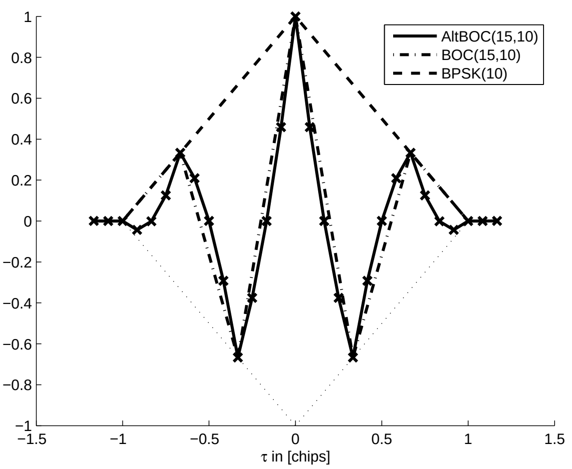

Figure 5. The ACF of the Galileo E5 AltBOC signal and its confrontation with ACF of other GNSS counterparts. The $\mathcal{R}_{\mathcal{E}5}(\tau)$ is computed under assumptions: $P = 1$, the pulse $g_{T_s}(t)$ is rectangular with T_s duration, consequently $\rho_{g_{T_s}}(\tau)$ has triangular shape. This corresponds with infinite channel bandwidth.

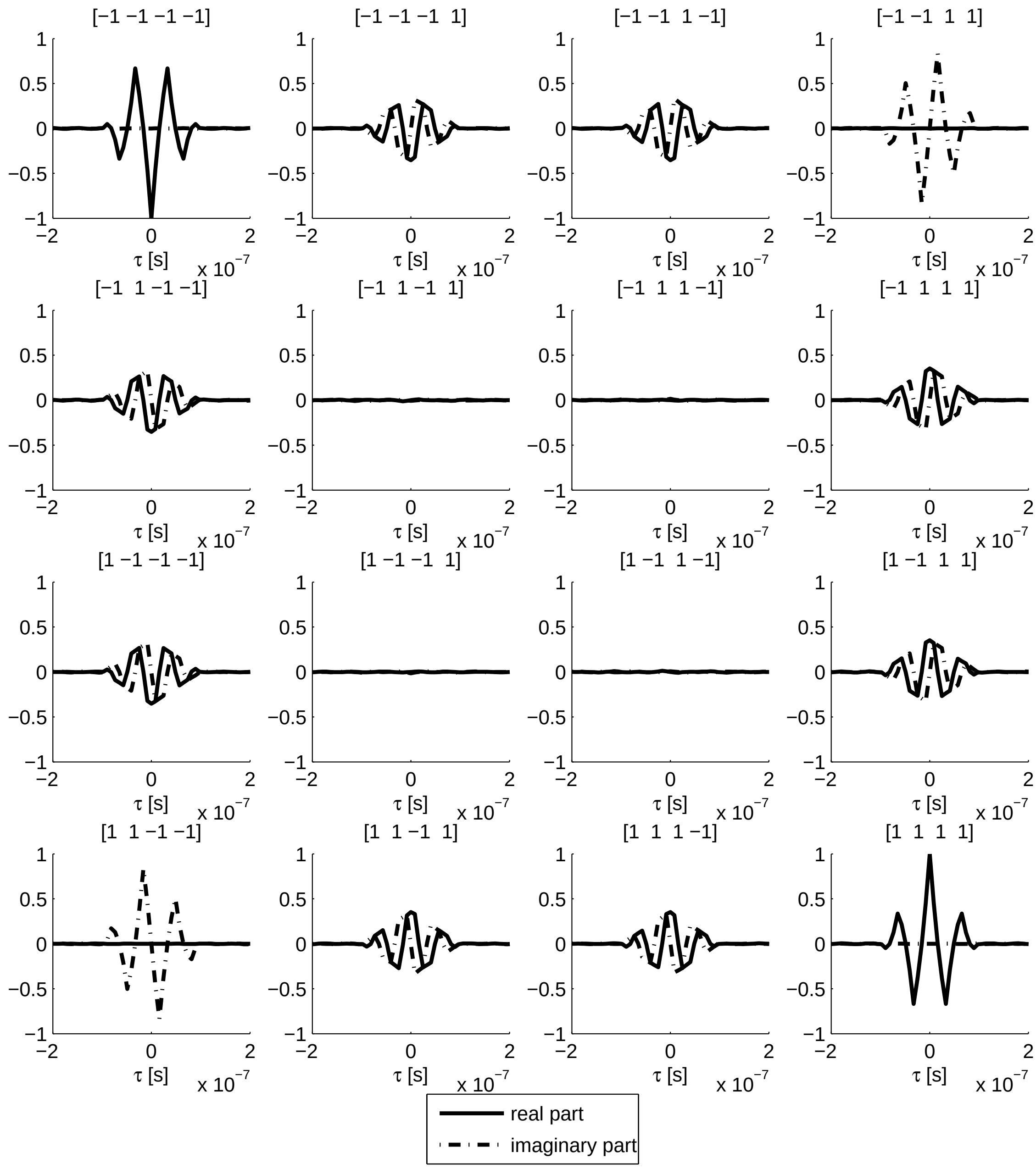

Figure 6. The CCF of Galileo E5 AltBOC signals for various secondary sequences (dis)agreement. Real part of CCF is drawn with solid line, the imaginary part with dot-and-dash line. The charts are computed under assumptions: integration time $T_I = 1\text{ms}$, ${}^sP = {}^rP = 1$, infinite channel bandwidth

In case, where the secondary sequence synchronization is done, there are still four possibilities of CCF shape due to navigation data bits uncertainty in two AltBOC input branches. This corresponds with the quarter of Fig. 6. Thus, the DLL detector which fully utilizes wideband E5 AltBOC signal processing has to compute the correlation for all data bits possibilities (have to suppose both data bits polarity in AltBOC input branches). Then the detector logic should decide which correlator outputs are correct and use them for NCO driving.

Finally, we add that the Fig. 5 and Fig. 6 were numerically computed in *Matlab* and confronted with analytically derived formula in *Mathematica*. The perfect fit proves the correctness of both equations (31) and (32)

V. Conclusion

This paper presents the analytical derivation of the CCF of Galileo E5 AltBOC signals for arbitrary difference in secondary sequences chips (and also navigation data bits uncertainty). The derivation was based on signal decomposition into several tiers and their separated investigation. As a consequence the derived formulas depend on secondary sequences CCF and subcarriers CCF. The matrix of CCF subcarriers was evaluated and was provided in graphic and tabular form for comfortable using. The only work to do for E5 AltBOC CCF evaluation is a computation of secondary sequences CCF. Since the secondary sequences length involved into integration is usually small, such computation can be done easy.

The straightforward result issued from derived formulas is ACF of Galileo E5 AltBOC signal. This ACF was computed and shown with other connected GNSS counterpart ACF into common chart.

The all CCF possibilities for 1ms integration time were shown. This provides base information how to design the DLL detector which fully utilize E5 signal bandwidth. Since the knowledge of navigation data bits cannot be supposed, there are four possible shapes of CCF (the correct secondary sequence synchronization is assumed). Only one of them should be use for the detector output computation.

Acknowledgment

Research described in the paper was financially supported by the Czech Ministry of Education under research program MSM 6840770014.

References

[1] Sleewaegen, J. M. – Wilde, W. – Hollreiser, M.: *Galileo AltBOC Receiver.* [online] Available from: http://www.septentrio.com/papers/GallileoAltBOC_paperFinal.pdf

[2] OS SIS ICD, Draft 1. *Galileo Open Service, Signal In Space Interface Control Document.* European Space Agency / European GNSS Supervisory Authority. February 2008.

[3] Kačmařík, P. – Kovář, P.: *GNSS Signals Characteristics.* In Proceedings of 17th International Conference Radioelektronika 2007. Brno: FEEC BUT, 2007, p. 199-204. ISBN 1-4244-0821-0.